# Building Chemical Intuition About Physicochemical Properties of C8-Per-/Poly-fluoroalkyl Carboxylic Acids Through Computational Means

Jonathan P. Antle,<sup>a</sup> Michael A. LaRock,<sup>b</sup> Zackary Falls,<sup>c</sup> Carla Ng, <sup>d</sup> G. Ekin Atilla-Gokcumen,<sup>a</sup> Diana S. Aga,<sup>a</sup> and Scott M. Simpson<sup>b\*</sup>

#### **AUTHOR ADDRESS**

- <sup>a</sup> Department of Chemistry, University at Buffalo, the State University of New York (SUNY) Buffalo, NY 14260, United States
- <sup>b</sup> Department of Chemistry, St. Bonaventure University, St. Bonaventure, NY 14778, United States
- <sup>c</sup> Department of Biomedical Informatics, Jacobs School of Medicine and Biomedical Sciences, University at Buffalo, Buffalo, NY 14203, United States
- <sup>d</sup> Department of Civil & Environmental Engineering, University of Pittsburgh, PA 15261, United States
- \* Corresponding Author: email:ssimpson@sbu.edu, phone: 716-307-1706

#### **KEYWORDS**

Per-/poly-fluoroalkyl substances, octanol-water partition coefficient, membrane-water partition coefficient, COSMO-RS, acid dissociation constant

#### ABSTRACT:

We have predicted acid dissociation constants (pK<sub>a</sub>), octanol-water partition coefficients (Kow), and DPMC lipid membrane-water partition coefficients (K<sub>lipid-w</sub>) of 150 different 8-carbon containing poly-/per-fluoroalkyl carboxylic acids (C8-PFCAs) utilizing COSMO-RS theory. Different trends associated with functionalization, degree of fluorination, degree of saturation, degree of chlorination, and branching are discussed based upon the predicted values for the partition coefficients. In general, functionalization closest to the carboxylic head group had the greatest impact on the value of the predicted physicochemical properties.

#### 1. Introduction

Within the last few decades, the scientific community has awakened to the threat that Per- and Polyfluorinated Alkyl Substances (PFAS) pose towards human and environmental safety. 1-4 These substances have been demonstrated to be immunopathogenic, carcinogenic, and in preliminary zebrafish studies, even teratogenic.<sup>3,5,6</sup> The daunting reality of this issue is that there exist over 8,000 PFAS substances across the global market for a wide range of applications. 7-10 However, very few of these chemicals have been tested for toxicity, despite the demonstrated health risks of some PFAS, or have had their physicochemical properties quantified, despite the need to understand their fate & transport. One of the major goals set out by the PFAS research community is the attainment of physicochemical properties. 11 These properties can be predictive of human and environmental effects and therefore a first entry point for toxicology and bioaccumulation investigation regarding PFAS. Since experimental tests for assessing chemical toxicity and quantification of physicochemical properties are difficult, costly, and time-consuming, useful data may not be available for years. Hence, there is a critical need to design standard platforms for assessing PFAS toxicity and physicochemical properties. <sup>11–15</sup> This deficiency in knowledge is only exacerbated by the chemical elusiveness of PFAS isolation from complex environmental and biological matrices paired with the limited availability of analytical standards for these compounds. 16,17 Unfortunately, these caveats makes the utilization of OSARs to predict physicochemical properties unreliable due to lack of experimental data. Therefore, computational means of predicting the physicochemical properties of PFAS will yield a powerful and relatively inexpensive method compared to wet lab approaches to understanding the overall

behavior of these types of substances and may allow for the development of preliminary risk assessment tools.

Physicochemical properties have been predicted within chemical accuracy by DFT, COSMO-RS, along with SPARC, Open structure-activity/property Relationship App (OPERA), EPI Suite, and machine-learning methods, for a variety of compounds, including PFAS. 14,18–29
Herein, we elect to utilize COSMO-RS models to predict relevant physicochemical properties.

Quantum mechanical calculations paired with COSMO-RS models present a reliable method to predict physicochemical properties. 28,30–32 This method is especially indicated for PFAS as fluorine chemistry exhibits hyper conjugative effects and novel chemical properties that may often conflict with common organic chemical intuition. 33 At this point, no reliable forcefield parameters for PFAS exist, which further supports QM calculations as the computational method of choice. 34

This study is motivated by the sheer chemical diversity available to the PFAS family, and the urgency to understand and prioritize risk assessment of these ubiquitous pollutants. Since the emergence of fluorinated alternatives including (1) shorter-chain homologues of legacy PFAS, (2) functionalized polyfluoropolyethers (PFPEs), and (3) sulfonic/phosphoric acids, very few studies have reported their physicochemical, bio-accumulative, toxicological, or bio-transformative properties. Additionally, precursor compounds are on the radar as potentially unaccounted-for sources of PFAS exposure. Little information is readily available on any of the pertinent properties for these emerging in pollutants.

Given the ionogenic nature of PFAS, the acid dissociation constant (pKa) is an important physicochemical property to know but proves to be difficult to obtain experimentally or is unknown for emerging PFAS. <sup>19,28,42</sup> Often, researchers assume that the pK<sub>a</sub> of different PFAS is

low, meaning they only need to consider the anionic form of the molecule. However, experimental values of  $pK_a$  for even the most well-studied PFAS are highly debated. The value of pKa also gives insight into the partitioning behavior of these molecules, i.e. are the molecules expected to be anionic or neutral. The  $pK_a$  values of per-/poly-fluorinated carboxylic acids (PFCAs) has been predicted by COSMO-RS models, in-addition to other models.  $pK_a$  values of per-/poly-fluorinated carboxylic

One parameter for gauging lipophilicity of a compound is the octanol-water partition coefficient (K<sub>OW</sub>). K<sub>OW</sub> has been used to gauge the relative bioaccumulation of lipophilic compounds which may yield insight into the bio accumulative potential and base-line toxicity for some compounds. However, K<sub>OW</sub> coefficients prove to be difficult to quantifywith high uncertainty as a result due to a lack of the aforementioned standards, due to their surfactant behavior, or even a lack of standardized methods to conduct experiments. 12,15

Experimental methods include using artificial membrane columns, and computationally using COnductor like Screening MOdel for Realistic Solvents (COSMO-RS) theory or molecular dynamics (MD) simulations. <sup>24,42,46,51–54</sup> Higher concentrations of PFAS have been measured in tissues that have higher amounts of phospholipids than neutral lipids. <sup>55,56</sup>

Membrane partitioning of PFAS has also been studied in bacteria.  $^{51}$  These studies have identified the phospholipid bilayer as an important reservoir for PFAS accumulation. Therefore, membrane-water partition coefficients ( $K_{lipid-w}$ ) using phospholipid-derived lipid bilayers are of relative importance for understanding the partitioning behavior and accumulation of PFAS.

Herein, we present pK<sub>a</sub>, log  $K_{OW}$ , & log  $K_{lipid-w}$  values calculated from COSMO-RS theory of over 150 different per-/poly-fluoroalkyl carboxylic acids (PFCAs) that contain 8

carbon atoms. These selected molecules have a wide range of different functionalization, bond saturation, and degree of fluorine/chlorine saturation.

# 2. Computational Details

All molecules discussed in this study were constructed using Avogadro Software and initially optimized with UFF forcefield.<sup>57</sup> Conformers were produced using Vconf software, with an energy cutoff set at 1-5 kcal/mol.<sup>58</sup> A maximum of 50 conformers were produced and optimized by DFT methods. DFT geometry optimization calculations were performed using TURBOMOLE software package<sup>59,60</sup> with the BP86 functional<sup>61,61</sup> and the def-TZVP basis set<sup>62</sup> from the TURBOMOLE basis set library. The BP86 functional was selected as this was utilized in the parameterization in the physicochemical predictions of COSMOtherm<sup>63</sup>. Both neutral forms and anionic forms were optimized for the PFCAs. We highlight that COSMO-RS can be used to predict physiochemical properties of ions whereas it is impossible for other predictive methods.<sup>53</sup>

Herein, we highlight the basics of COSMO-RS theory but highly we suggest the readers to review the strong literature associated with COSMO-RS.  $^{32,63-66}$  Our previously mentioned DFT calculations are utilized to generate a  $\sigma$ -profile of each molecule. These  $\sigma$ -profiles are then utilized to calculate chemical potentials ( $\mu$ ) utilizing COSMO-RS theory via the COSMOtherm software package. Finally, these  $\mu$  are utilized in the calculation of the different physicochemical properties.

#### 2.2 Calculating acid dissociation constants ( $pK_a$ ):

COSMOtherm software was utilized to calculate the acid dissociation constant (pK<sub>a</sub>). The COSMOtherm BP TZVP 19 parametrization was used for the calculation of pK<sub>a</sub>. Optimized

structures of the anionic form (missing a proton) and the neutral forms we utilized in the COSMOtherm calculation. The pKa was calculated using a weighted Boltzmann distribution that accounts for all entered conformers. This COSMO-RS methodology has been tested with a variety of 64 organic and inorganic acids, approximating the error of the pKa values to be  $\pm 0.49$  logarithmic units. Utilizing our methodology, we calculate a pKa value for perfluoro octanoic acid (PFOA) of 0.709. This matches the value calculated by Goss, and falls within the range of the debated experimental values of sub-zero to 3.8. In our calculations, we assume that the carboxylic acid functional group will be deprotonated to form the anion, which may not necessarily be true given the strange behavior of fluorinated compounds and the wide diversity of functional groups.  $^{23,43,45,69-71}$ 

# 2.3 Calculating water-octanol partition coefficient (log Kow):

COSMOtherm software was utilized to calculate the octanol-wet water partition coefficient (log  $K_{\rm OW}$ ) for the anionic forms of the molecules. Wet octanol was chosen for the nonpolar phase as this more closely approximates experimental conditions. The COSMOtherm  $BP_TZVP_19$  parametrization was used for log  $K_{\rm OW}$  calculations. This method has been utilized previously to reliably predict log  $K_{\rm OW}$  for varying neutral and anionic PFAS species, and other compounds. The log  $K_{\rm OW}$  was calculated using a weighted Boltzmann distribution that accounts for all entered conformers.

#### 2.4 Calculating lipid bilayer partition coefficients (log $K_{lipid-w}$ ):

COSMOmic,  $^{72}$  as part of the COSMOtherm suite, was utilized to calculate the phospholipid membrane-water partition coefficient (log  $K_{lipid-w}$ ). Specifically, the weighted partition ratio between water and a hydrated zwitterionic 1,2-dimyristoyl-sn-glycero-3-

phosphocholine (DMPC) phospholipid bilayer were computed. The results of molecular dynamics (MD) generated by Jakobtorweihen et al. were utilized in our COSMOmic calculations to simulate our lipid membrane.<sup>73</sup> For the general procedure associated with COSMOmic we refer the reader to the work of Jakobtorweihen et al. and Klamt et al.<sup>72,73</sup> However, we prodive a general overview of COSMOmic herein.

COSMOmic utilizes the same input as COSMO-RS, the  $\sigma$ -profile obtained from DFT geometry optimization calculations. This includes the solute molecule (in our case a PFAS of interest), solvent molecule (water in this study), and a single lipid molecule. COSMOmic differs from COSMO-RS in that a system is divided up into smaller subsystems then summed over these divisions. The system that is divided up is obtained from MD simulations of the anisotropic system (lipid+water). A solute molecule is then placed within these layers and a chemical potential is calculated. A free energy profile is then calculated based upon these chemical potentials. From here, the free energy profile is then utilized to calculate the log  $K_{lipid-w}$  value.

The COSMOtherm BP\_TZVP\_C30\_1401 parametrization was used for log K<sub>lipid-w</sub> calculations. The same membrane dipole potential utilized by Bittermann et al. was utilized in this study.<sup>74</sup> This methodology has been shown to be effective at calculating DPMC lipid membrane-water partition coefficients for PFAS.<sup>42,53</sup>

#### 3. Results and Discussion

# 3.1 Error Analysis of COSMO-RS & COSMOtherm

To demonstrate the accuracy and utility of COSMO-RS/COSMOtherm and COSMOmic, we report pKa, and log K<sub>OW</sub> values for various PFAS reported in the literature. The comparison to experimental values for PFAS tends to be limited/problematic. <sup>12,43,45</sup> Table 1 contains a comparison of experimental and theoretical log K<sub>OW</sub> values for a series of fluorotelomer

alcohols. Table 2 contains pKA values for a series of PFCAs. The root-mean absolute error (MAE) and root-mean square error (RMSE) indicate that our calculations show comparable results to prior COSMOtherm calculations and OPERA calculations, similar to what others have shown. However, the MAE and the RMSE values may be skewed due to the larger number of pKa values for so-called "short-chain" PFAS over "long chain" PFAS. A more detailed error analysis associated with the value contained herein, and the difference in experimental techniques can be found in the Supporting Information. For more information about the performance of COSMOmic for the calculation of K<sub>lipid-w</sub> please refer to the work by Jakobtorweihen et al. and Klamt et al. T2,73

Table 1: Octanol-water partition coefficients (log  $K_{OW}$ ) estimates and previously determined experimental values. The mean absolute error (MAE) and root-mean square error (RMSE) is indicated.

FTOH	log Kow (experiment) <sup>75</sup>	log Kow (calculated, us)	log Kow (calculated, previous) <sup>24</sup>	log Kow (OPERA)
4:2 FTOH	3.28	2.65	-	3.27*
6:2 FTOH	4.54	3.82	3.17	3.47, 3.64*
8:2 FTOH	5.58	4.97	4.84	6.07, 5.07*
10:2 FTOH	6.63	6.14	7.45	7.74, 7.09*
MAE	-	0.61	0.98	0.89, 0.47*
RMSE	-	0.62	1.02	0.93, 0.57*

<sup>\*</sup> Calculated by OPERA 2.6 on the EPA CompTox Chemical Dashboard v2.2.19

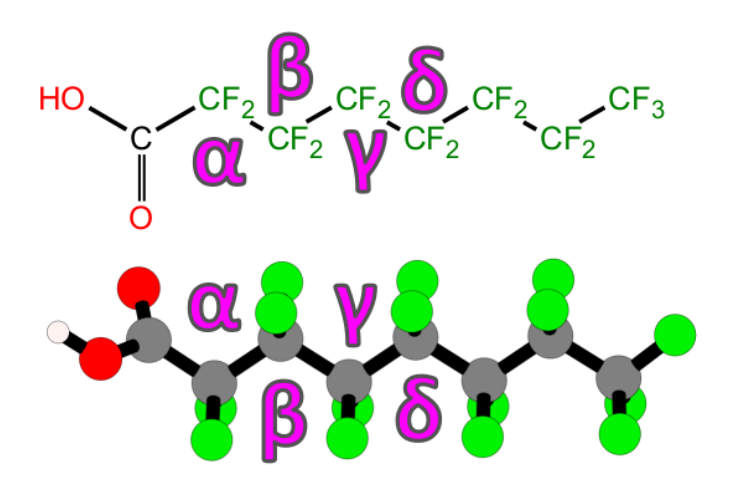
Table 2: Acid dissociation constants  $(pK_a)$  estimates and previously determined experimental values. The mean absolute error (MAE) and root-mean square error (RMSE) is indicated

PFCA	pK <sub>a</sub> experiment	pK <sub>a</sub> (Calculated, us)	pK <sub>a</sub> (Calculated, previous) <sup>24</sup>	pK <sub>a</sub> (OPERA) <sup>24,*</sup>
PFDA	2.58 <sup>70</sup>	0.78	0.47	0.40
PFOA	3.80 <sup>24,44</sup>	0.80	0.36	0.34
	1.01 <sup>24,76</sup>	0.80	0.36	0.34
	1.31 <sup>77</sup>	0.80	0.36	0.34
	2.50 <sup>24,24</sup>	0.80	0.36	0.34
PFPeA	0.85 <sup>24</sup>	0.75	0.43	0.80
	0.23 <sup>70</sup>	0.75	0.43	0.80
	0.23 <sup>70</sup>	0.75	0.43	0.80
	0.37 <sup>70</sup>	0.75	0.43	0.80
	0.54 <sup>77</sup>	0.75	0.43	0.80
PFBA	0.64 <sup>24</sup>	0.72	0.55	-0.21
	0.48 <sup>70</sup>	0.72	0.55	-0.21
	0.36 <sup>70</sup>	0.72	0.55	-0.21
	0.38 <sup>70</sup>	0.72	0.55	-0.21
	0.37 <sup>77</sup>	0.72	0.55	-0.21
PFPrA	0.32 <sup>24</sup>	0.83	0.03	0.81
	0.38 <sup>70</sup>	0.83	0.03	0.81
	0.34 <sup>70</sup>	0.83	0.03	0.81
	0.29 <sup>70</sup>	0.83	0.03	0.81
	0.44 <sup>77</sup>	0.83	0.03	0.81
TFA	-0.30 <sup>19</sup>	0.95	0.60	0.72
	$0.49^{24}$	0.95	0.60	0.71
	0.35 <sup>70</sup>	0.95	0.60	0.71
	0.26 <sup>70</sup>	0.95	0.60	0.71
	0.24 <sup>70</sup>	0.95	0.60	0.71
MAE		0.661	0.582	0.777
RMSE	DED 4 2 (	0.420	0.485	0.572

Calculated by OPERA 2.6 on the EPA CompTox Chemical Dashboard v2.2.19

# 3.2 Diversity of PFCAs Studied

Herein, we only considered fluorinated carboxylic acid molecules containing a total of 8 carbon atoms, which we term C8-PFCAs. 150 different C8-PFCAs were optimized and had their physicochemical properties calculated. Throughout this work we will refer to different positions on the per-fluorinated chain utilizing schematic 1, as reference to the carboxylic headgroup.



Schematic 1: (top) A skeletal structure & (bottom) cartooned representation of PFOA indicating the  $\alpha$ ,  $\beta$ , $\gamma$ , &  $\delta$  positions on the per-fluorinated chain with respect to the carboxylic head group. White/red/grey/green spheres represent hydrogen/oxygen/carbon/fluorine atoms, respectively.

The functional groups and the number of molecules that fall within that class that were considered in this study are listed in Table 3. A molecule with multiple functional groups would be considered to fall within multiple categories associated with functional group. For example, a C8-PFCA containing an ester and a thiol would count once under the thiol category and once under the ester category. We assume that each C8-PFCA is saturated with fluorine atoms, unless it falls under the "unsaturated" category, indicating that at least 1 fluorine atom has been replaced by a hydrogen atom. The "chlorinated" category indicates that the C8-PFCA that at least 1 fluorine atom has been replaced by a chlorine atom. The "branching" category indicates that the C8-PFCA molecule is not linear, such as 2-trifluoromethyl-perfluoroheptanic acid. The category "ring" indicates that a benzylic ring is contained within the structure of the C8-PFCA molecule. Each individual C8-PFCA's skeletal structure and SMILES can be found in the Supporting Information (SI).

While there are many comparisons that could be made with this data, we focus on major aspects we find interesting. While accuracy of the methodology is important, we would like to remind the reader that we are interested in the trends associated with functionalization of these molecules.<sup>78</sup> Herein, we discuss relevant trends that we believe are of importance to the reader but encourage the reader to utilized the files we generate to investigate additional trends. We freely provide the COSMOtherm files to anyone with internet access.<sup>79</sup>

Table 3: The functional group category and number of molecules associated with the category. An example skeletal structure of a representative member of the functional group category is also included.

Functional Group Category	# Of Molecules (N)	Example Molecule
Alkene	18	$\begin{array}{c} \text{O} \\ \text{OH} \end{array}$
Alkyne	5	$\begin{array}{c c} \text{O} & \text{CF}_2 & \text{CF}_2 & \text{CF}_3 \\ \text{OH} & \text{OH} & \text{CF}_2 & \text{CF}_3 \\ \end{array}$
Anhydride	3	$ \begin{array}{c c} O & CF_2 & CF_2 & CF_2 \\ & & & \\ O & & & \\ \end{array} $
Branching	49	$ \begin{array}{c} \text{O} \\ \text{OH} \\ \text{CF}_{2} \\ \text{CF}_{3} \\ \end{array} $
Carbonyl	16	$ \begin{array}{c} \text{O} \\ \text{OH} \end{array} $
Chlorinated	13	$\begin{array}{c c} CI & CF_2 & CF_2 & CF_2 \\ \hline \\ OH & CI & CF_2 & CF_2 & CF_2 \end{array}$
Ester	34	$ \begin{array}{c ccccccccccccccccccccccccccccccccccc$
Ether	16	$\begin{array}{c} \\ \\ \\ \\ \\ \\ \\ \\ \\ \\ \\ \\ \\ \\ \\ \\ \\ \\ \\$

Ring	8	FC F S.1
Thioester	9	$\begin{array}{c ccccccccccccccccccccccccccccccccccc$
Thioether	14	$\begin{array}{c ccccccccccccccccccccccccccccccccccc$
Thioketone	3	$\begin{array}{c c} O & CF_2 & CF_2 & CF_2 \\ OH & S & CF_2 & CF_2 & CF_3 \end{array}$
Thiol	15	$ \begin{array}{c} \text{O} \\ \text{CF}_2 \\ \end{array} $
Unsaturated	37	$ \begin{array}{c} \text{O} \\ \text{OH} \\ \end{array} $

# 3.3 pKa PFCAs

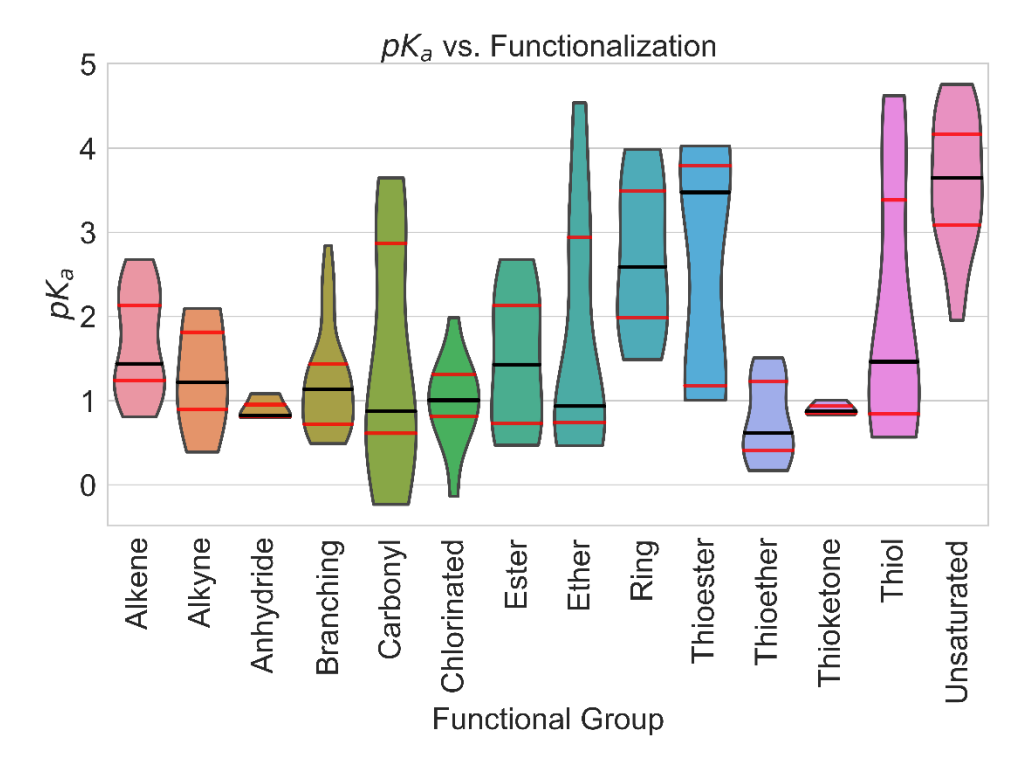


Figure 1: Violin plots of the  $pK_a$  versus the functional group categories. The median  $pK_a$  value is marked with a black line while the  $1^{st}$  and  $3^{rd}$  quartiles are marked with a red line.

A violin plot of the log pKa values of the 150 C8-PFAS vs. their functionalization can be seen in Figure 1. The average predicted pKa value for the 150 C8-PFCAs was 1.704 with a maximum of value 4.758, a minimum value of –0.232, and a standard deviation of 0.992 logarithmic units. Of the molecules studied, PFCAs with a thiol group or ether functional group had the largest range of pKa values. Of the molecules studied, thioesters and unsaturated C8-PFCAs had the highest average pKa values while C8-PFCAs functionalized with carbonyls, anhydrides, and thioethers had the lowest average pKa values.

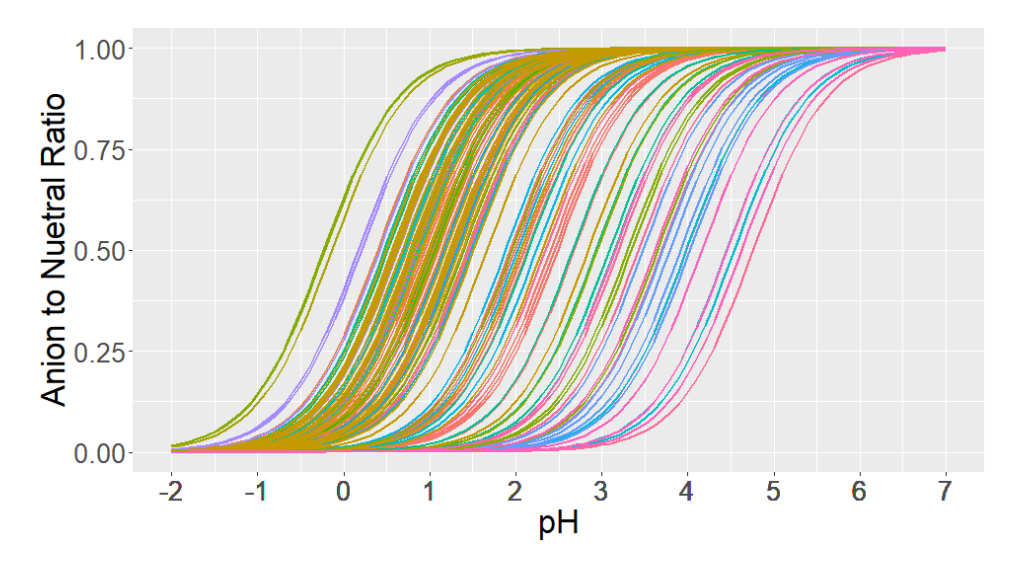


Figure 2: Relative amount of the anionic form of the C8-PFCAs versus the pH. The colors of the lines/area of the lines are associated with different functional groups.

Those looking to study C8-PFCAs in their anionic form will need to consider utilizing a basic media to ensure 100% conversion to the anionic form, especially when considering a mobile phase of high-performance liquid chromatography (HPLC). However, according to our predictions the majority of the C8-PFCAs should be converted completely to their anionic state at a pH=7. To demonstrate this, we utilize the acid dissociation constant to determine the relative amount of anion (Anion to Neutral Ratio) of all 150 C8-PFCAs as a function of pH in Figure 2. We assume the C8-PFAS are in low ionic strength environment to have the activities of the C8-PFCAs approach their concentrations in our calculations of %anion. However, commonly used treatments of the mobile phase to reduce pH should be approached cautiously as some of our tested C8-PFCAs have higher than the previously mentioned average pK<sub>a</sub> values. For example, formic acid/phosphate/acetic acid buffers with pK<sub>a</sub> values of 3.8/2.1/4.8, respectively, would result in an appreciable amount of neutral C8-PFCAs in solution as predicted for our 150 C8-PFCAs.

Initially, one may elect based upon the predicted  $pK_a$  value for the majority of the explored C8-PFAS is lower than 2 logarithmic units, one would only need consider the anionic forms of the molecules when calculating the other physicochemical properties herein (log  $K_{OW}$  and log  $K_{lipid-w}$ ), given that at a pH of 7 or greater would permit the dominance of the anionic forms for the majority of the molecules. However, to determine if this is indeed a valid approximation we utilized COSMO-RS theory to calculate the Gibbs free energy of solvation ( $\Delta G_{solv}$ ) for the anionic and the neutral forms of each molecule with water/octanol/1,2-dimyristoyl-sn-glycero-3-phosphocholine (DMPC) as solvents. To compare the difference in the  $\Delta G_{solv}$  between the anionic form and the neutral form of each molecule we introduce a convention to compare the change in  $\Delta G_{solv}$  via equation 1:

$$\Delta(\Delta G_{\text{solvent}}) = \Delta G_{\text{solv}}(\text{neutral}) - \Delta G_{\text{solv}}(\text{anion})$$
[1]

Where  $\Delta G_{solv}$  (neutral) is the Gibbs energy of solvation of the neutral form of the C8-PFCA,  $\Delta G_{solv}$  (anion) is the Gibbs energy of solvation of the anionic form of the C8-PFCA, and  $\Delta (\Delta G_{solvent})$  is the difference between the two previously mentioned values. Therefore, a positive  $\Delta (\Delta G_{solvent})$  indicates that the anionic form of the molecule is more thermodynamically favorable while a negative value indicates that the neutral form is more preferred.

The results of these calculations can be seen in Figure 3. For all cases considered herein,  $\Delta(\Delta G_{solvent})$  is lower for the anionic PFCA over the neutral form in H<sub>2</sub>O and octanol. However, for DMPC the  $\Delta G_{solvent}$  was determine to be lower for neutral form for the majority of the 150 molecules. Predicted values for all partitioning coefficients and relevant thermodynamic properties are contained within the supporting information for both the anionic and the neutral forms of each PFCA.

However, is the neutral form that is the most prevalent as the molecule passes through the lipid bilayer? To answer this question, we calculate the Gibbs free energy profile of PFOA (Figure 3). These Gibbs free energy profiles can elucidate the distribution of the neutral/anionic/cationic forms of the same molecule at different depths within the phospholipid membrane. FFOA is a good representative case for the general behavior of the studied C8-PFACs. Generally, the anionic form sorb on the "exterior" side of the headgroup of the DMPC near the positively charged quaternary amine while the neutral form of PFOA sorb to the aliphatic chain contained within the lipid.

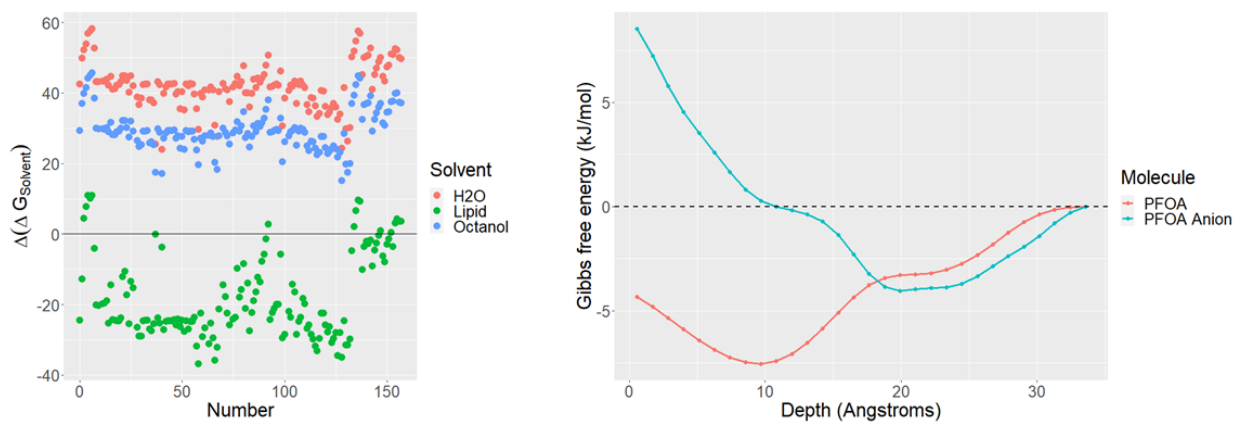


Figure 3: (left) Plot of  $\Delta(\Delta G_{solvent})$  vs. the molecule's index number (Number) of the octanoic acids in water, the DMPC lipid, and octanol. (right) Gibbs free energy profile for the (black/red line) neutral/anion form, respectfully, of PFOA traversing a DPMC lipid layer.

A comparison between the log  $K_{OW}$  and the log  $K_{lipid-w}$  values for the anionic and the neutral forms of the molecules are contained within the Supporting Information. There is a general linear relationship between the anionic and neutral properties ( $R^2$ =0.77/0.66 for log  $K_{OW}/K_{lipid-w}$ , repectively). While the values associated each form differ by multiple logarithmic units, the general trends associated with each form should be retained.

#### 3.3.1 p $K_a$ and Fluorination

Unsurprisingly, the degree of fluorine saturation plays a large role in the value of the pK<sub>a</sub>. To investigate this, we consider a series of C8-PFAS that vary with fluorine saturation (molecules #0 to #7). Generally, as the degree of fluorination is decreased the pK<sub>a</sub> increases. However, position relative to the headgroup makes a large impact. For example, comparing the pK<sub>a</sub> value of molecule #6, where the only fluorinated carbon is on the opposite end of the 8-membered chain, to molecule #7, where the only fluorinated carbon is the  $\alpha$ -carbon relative to the carboxylic head-group, there is a difference in pK<sub>a</sub> values of  $\approx$  2.3 logarithmic units (4.623/2.345 for molecule #6/#7, respectively).

## 3.3.3 pK<sub>a</sub> for Fluorinated Rings

Upon inspection of the ortho-/meta-/para-isomers of trifluoromethyl-tetrafluorobenzocid acid, the further away the trifluoromethyl group is from the carboxylic head-group on the phenyl ring the lower the  $pK_a$  value. The predicted values were 2.02/2.24/1.88 for the o-/m-/p-isomer, respectively. The inductive effects associated with different positions of trifluoromethyl group could be the reason for this change.

#### 3.4 Log Kow of C8-PFCAs

As previously established, only the anionic forms of the 150 C8-PFCAs were considered when calculating the  $\log K_{OW}$  values. The  $\log K_{OW}$  values for the neutral form of the C8-PFCAs were also calculated but will only be reported in the Supporting Information.

A more positive log K<sub>OW</sub> value indicates favoritism for partitioning into the octanol phase while a more negative value indicates favoritism to partition into the water phase. The average predicted log K<sub>OW</sub> value for the anionic form of the 150 C8-PFCAs was –3.787. This indicates a preference for anionic forms of C8-PFCAs to partition into water over octanol, generally. A

maximum log K<sub>OW</sub> value of 0.010, a minimum value of –7.167, and a standard deviation of 1.158 logarithmic units was predicted. A violin plot of the log K<sub>OW</sub> values of the 150 C8-PFAS vs. their functionalization can be seen in Figure 4.

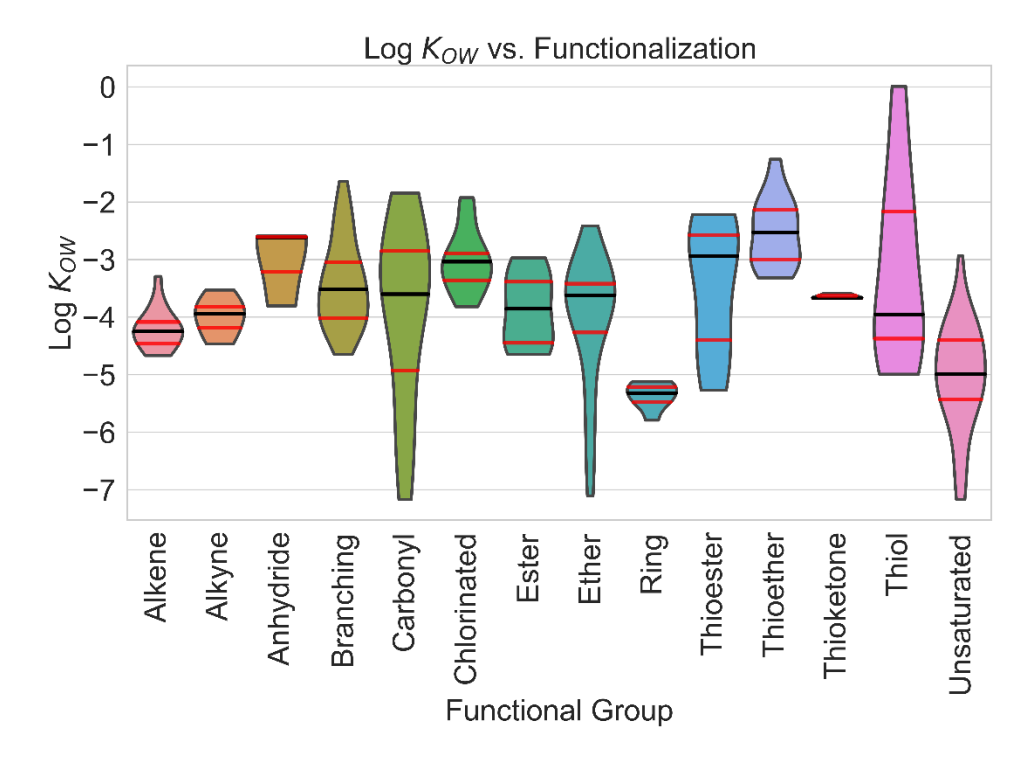


Figure 4: Violin plots of the log Kow versus the functional group categories. The median log Kow value is marked with a black line while the 1<sup>st</sup> and 3<sup>rd</sup> quartiles are marked with a red line.

Interestingly, the only category of C8-PFAS that ventured closely to having equal favoritism of water to octanol were two C8-PFCAs with a thiol functional group. There were molecules #37 and #40 with a log  $K_{OW}$  value of -0.479 and 0.010, respectively. The skeletal structures of these molecules can be found in the Supporting Information. Molecule #37 is an analogue to PFOA with a thiol functional group at the  $\beta$ -carbon with respect to the carboxylic group. Molecule #40 is similar to #37 with an additional thiol functional group at the  $\alpha$ -carbon.

The most hydrophilic of the tested C8-PFCAs tended to be functionalized with a carbonyl or ether groups. The most negative log K<sub>OW</sub> value of –7.167 was predicted for molecule #152.

This C8-PFAS has a carbonyl group at the  $\beta$ -carbon, with respect to the carboxylic head group, and is only fluorinated at the carbon at the opposite end of the molecule.

# 3.5 Log K<sub>lipid-w</sub> of C8-PFCAs

As previously established, only the anionic forms of the 150 C8-PFCAs were considered when calculating the log  $K_{lipid-w}$  values. The log  $K_{lipid-w}$  values for the neutral form of the C8-PFCAs were also calculated but will only be reported in the Supporting Information.

A more positive log K<sub>lipid-w</sub> indicates a corresponds partitioning into the DPMC phospholipid membrane while a smaller value indicates partitioning into water. The average predicted log K<sub>lipid-w</sub> value for the anionic form of the 150 C8-PFCAs was 2.335 with a standard deviation of 0.559 logarithmic units. This indicates a preference for anionic forms of C8-PFCAs to partition into the DPMC lipid bilayer over water, generally. The same trend is predicted for the K<sub>lipid-w</sub> of the neutral forms of these molecules. A maximum log K<sub>lipid-w</sub> value of 4.357 and a minimum value of 1.025. A violin plot of the log K<sub>lipid-w</sub> values of the 150 C8-PFAS vs. their functionalization can be seen in Figure 5.

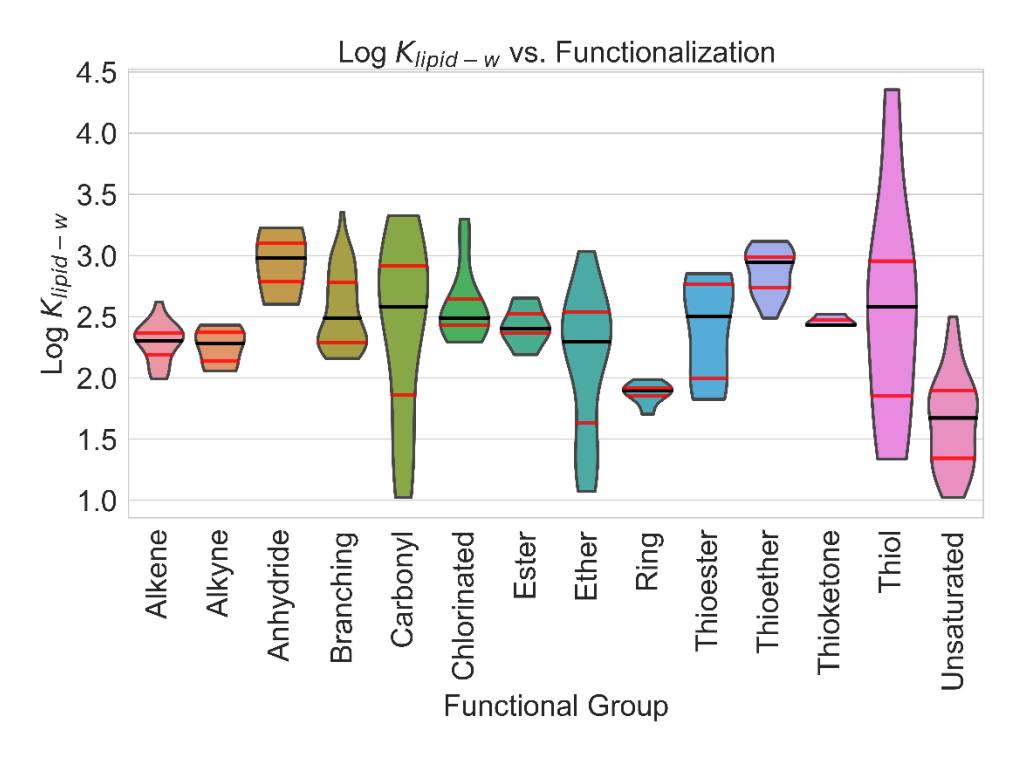


Figure 5: Violin plots of the log  $K_{lipid-w}$  versus the functional group categories. The median log  $K_{lipid-w}$  value is marked with a black line while the  $1^{st}$  and  $3^{rd}$  quartiles are marked with a red line. The units of log  $K_{lipid-w}$  are L(water)/kg(lipid).

The relationship between log  $K_{OW}$  and log  $K_{lipid}$  seems to have a linear correlation (Figure 6). In general, as log  $K_{lipid-w}$  increase so does Log  $K_{OW}$ . This provides justification for utilizing the octanol-water partition coefficient as an approximation to the phospholipid membrane-water partition coefficient. Log  $K_{lipid-w}$  has been correlated with cellular uptake and toxicity for PFAS. The PFACs with a residual larger than residual standard error of the regression (0.211 logarithmic units) were molecules #134, #138, #154 and #157. The compounds contained either an ether functional group (#134 & #138) or a thiol group (#154 & #157) and were not saturated with fluorine atoms. Their skeletal structures can be found in the Supporting Information. However, it should be pointed out that there are exceptions to this correlation, as we highlight in different sections and other studies have done before us, for PFAS.  $^{42,53}$ 

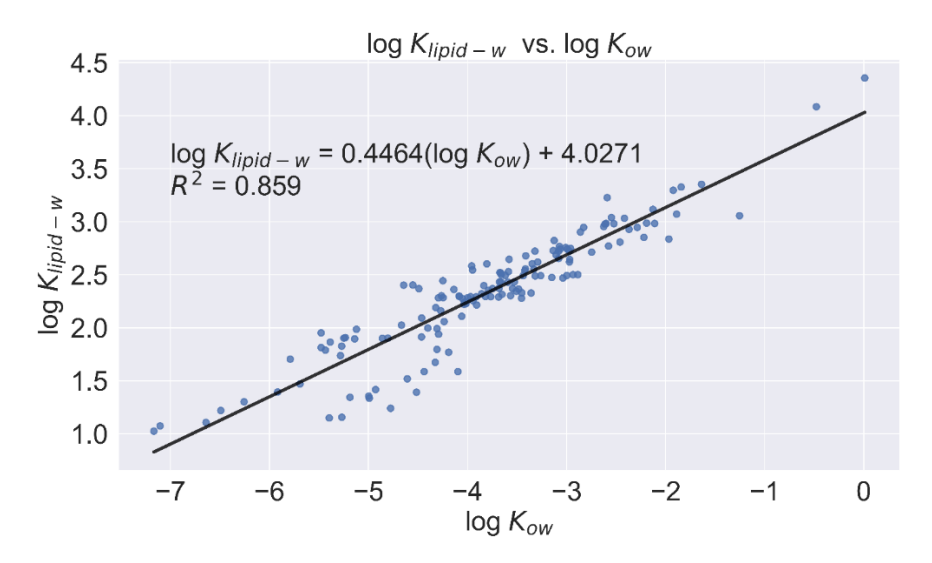


Figure 6: A plot of log  $K_{lipid-w}$  versus log  $K_{OW}$ . The units of log  $K_{lipid-w}$  are L(water)/kg(lipid).

# 3.6 Log K<sub>OW</sub> & log K<sub>lipid-w</sub> - Branching

The COSMO volume is associated with the volume of the molecule as calculated by COSMO-RS theory. 32,64 Therefore, we elect to utilize the COSMO volume as the properties associated with branching, as IUPAC naming can become quite cumbersome and/or uninformative with an exorbitant number of different analogs that could be generated by considering different branched isomers.

While the COSMO volume does not seem to have a linear relationship with the partition coefficients, trends can be pulled from Figure 7. Considering a series of perfluoroheptanonic acid with changing the position of a single trifluoromethyl group (molecules #41 to #45), the largest impact on the calculated partition coefficients was placement of trifluoromethyl group at the  $\alpha$ -position relative to the carboxylic head group. Placement of the trifluoromethyl group after this position seemed to have minor impact on the partition coefficients. The addition of an additional trifluoromethyl group to the  $\alpha$ -position decrease/increase the value of the log  $K_{OW}/\log K_{lipid-w}$ , respectively, when comparing molecule #41 to molecules #49 & #50.

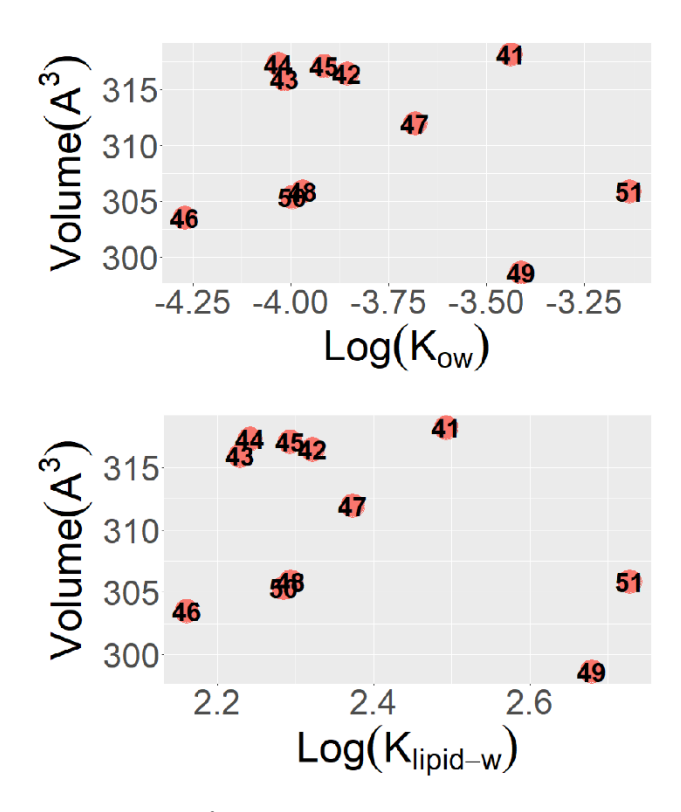
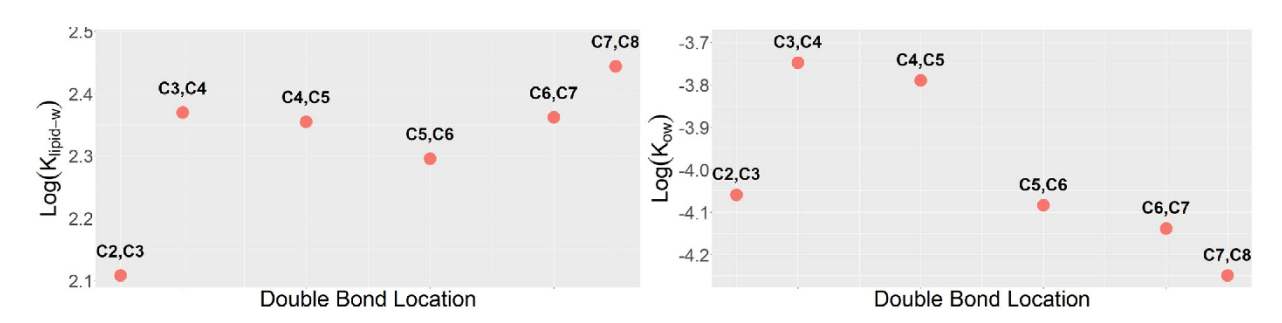


Figure 7: Plot of COSMO volume ( $\mathring{A}^3$ ) vs. (top) log Kow value or (middle) log K<sub>lipid-w</sub> value. The structures associated with the molecule number are indicated in the Supporting Information. The units of log K<sub>lipid-w</sub> are L(water)/kg(lipid).

#### 3.7 Log Kow & log Klipid-w - Saturation



Location	Structure	Location	Structure
C2,C3	F F F F OH	C5,C6	F F F OOH
C3,C4	F F F F OH	C6,C7	F F F F OH
C4,C5	F F F F OH	C7,C8	F F F F OH

Figure 8: Plot of predicted (top) log  $K_{OW}$  value or (middle) log  $K_{lipid-w}$  value vs. double bond location and (bottom) skeletal structures for the unsaturated C8-PFCAs. The units of log  $K_{lipid-w}$  are L(water)/kg(lipid).

Generally, the further away the alkene bond is from the carboxylic head group, the larger the log  $K_{lipid-w}$  values, as seen in Figure 8. The modification of saturation changed the predicted log  $K_{lipid-w}$  value by approximately 0.4 logarithmic units for the set of molecules considered in Figure 8. This indicates that the analogs become more lipophilic as saturation occurs further from the carboxylic head group for the tested C8-PFCAs. Interestingly, functionalization between C3 & C4 ( $\beta$  &  $\gamma$ ) and C4 &C5, ( $\gamma$  &  $\delta$ ) causes the log  $K_{OW}$  value to increase, showing deviation from the predicted log  $K_{lipid-w}$  values. Unsaturation impacted the predicted values of log  $K_{OW}$  by approximately 0.5 logarithmic units

### 3.8 Log Kow & log Klipid-w - Ethers and Thioethers

We have elected to modify the location of the bridging ether/thioether functional group, as seen in Figure 9. The thioether analogs have replaced the ether bond with a thioether functional group. The inclusion of a thioether or ether increases the log K<sub>OW</sub> and log K<sub>lipid-w</sub> values with respect to the value for PFOA. Interestingly, the placement of an ether functional group changes the predicted log K<sub>OW</sub> by 0.34 logarithmic units. However, the placement of a thioester group close to the carboxylic headgroup has a more pronounced effect, changing the predicted log K<sub>OW</sub> value by 1.8 logarithmic units. The replacement of an oxygen with a sulfur atom increases the log K<sub>OW</sub> value by approximately 1 logarithmic unit at the C2,C3 and C3,C4 positions, while the other positions have a much less pronounced impact. The position furthest away (C7,C8 position) had the least impact for thioethers. Interestingly, the opposite trend appears to be true for the ethers, the further from the headgroup the larger the partition coefficient.

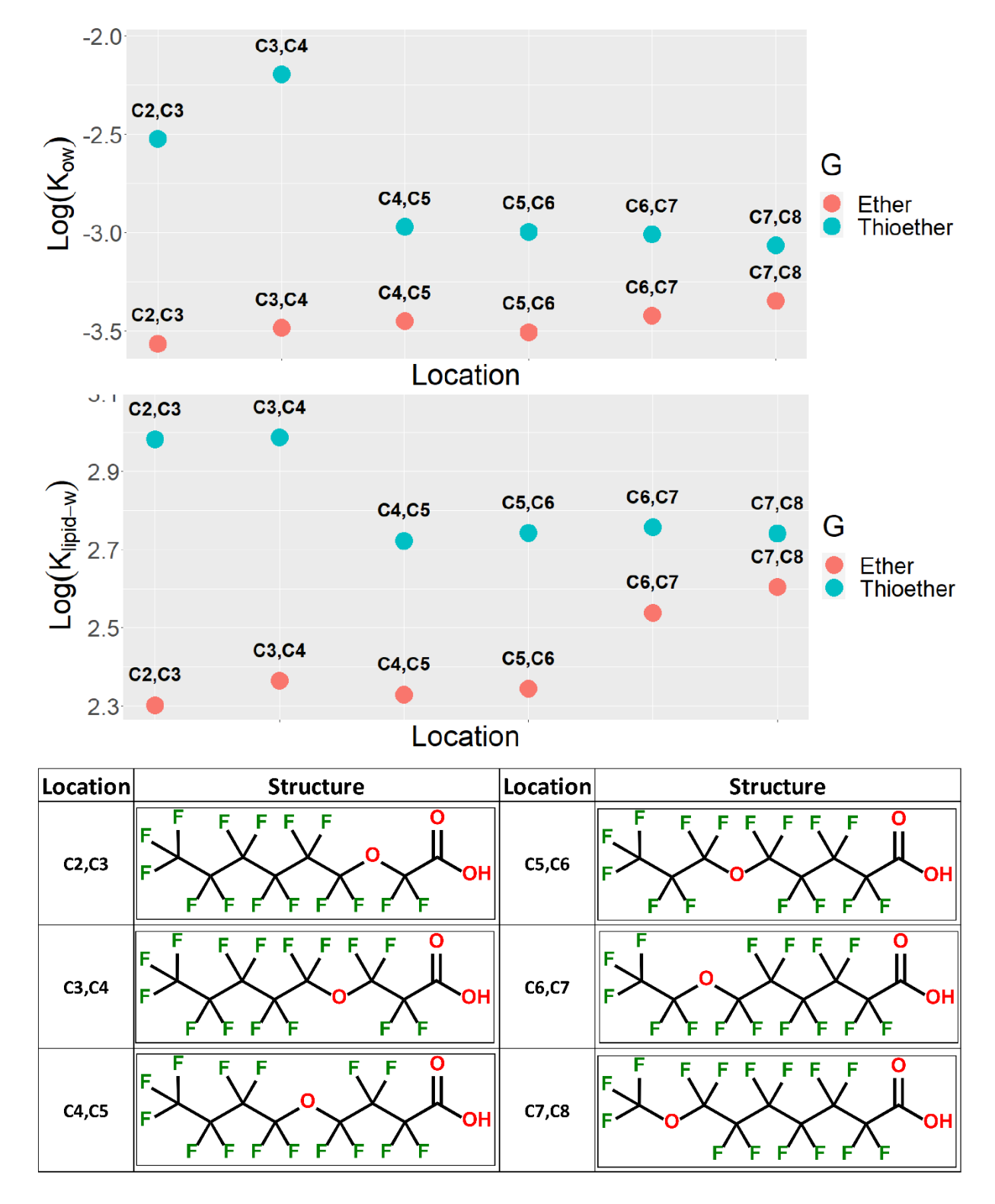


Figure 9: Plot of predicted (top) log  $K_{OW}$  value or (middle) log  $K_{lipid-w}$  value vs. functional group location of ether/thioether analogs and (bottom) associated skeletal structures for the C8-PFCAs. The units of log  $K_{lipid-w}$  are L(water)/kg(lipid).

# 3.9 Log Kow & log Klipid-w - Degree of Fluorination

The degree of fluorination is predicted to have a pronounced effect on both the log  $K_{\rm OW}$  and log  $K_{\rm lipid-w}$  values. As an example, we consider the different analogs of perfluorooctanoic acid (PFOA) with different degrees of fluorination. A plot of the partition coefficients and the structures considered are displayed in Figure 10. Generally, less fluorinated compounds are predicted to have a more negative log  $K_{\rm OW}$  value over more fluorinated compounds with a range of 1.747 logarithmic units. Log  $K_{\rm lipid-w}$  values were found to increase with fluorination with a range of 1.277 logarithmic units. Interestingly, the position of fluorination with respect to the carboxylic head group was found to change the log  $K_{\rm lipid-w}$  value by approximately 0.6 logarithmic units while log  $K_{\rm OW}$  only changed 0.165 logarithmic units when comparing molecule # 6 vs. molecule #7.

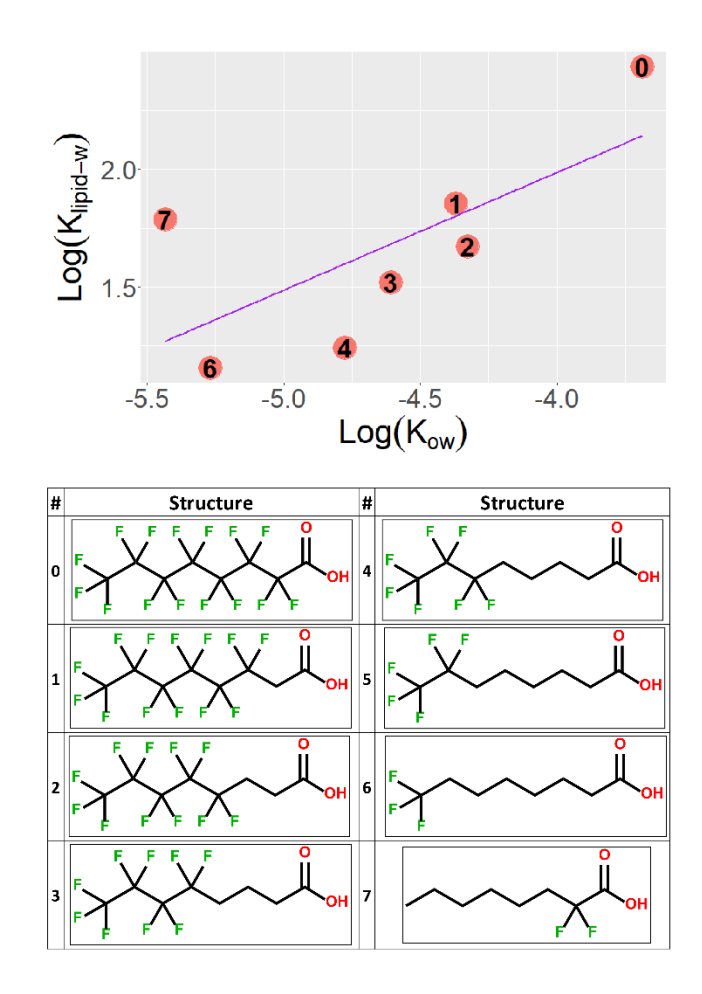


Figure 10: (Top) Plot of log  $K_{lipid-w}$  vs. log Kow of octanoic acids with varying degrees of fluorination and (bottom) associated skeletal structures C8-PFCAs. The units of log  $K_{lipid-w}$  are L(water)/kg(lipid).

# 3.10 Log Kow & log Klipid-w -Degree of Chlorination

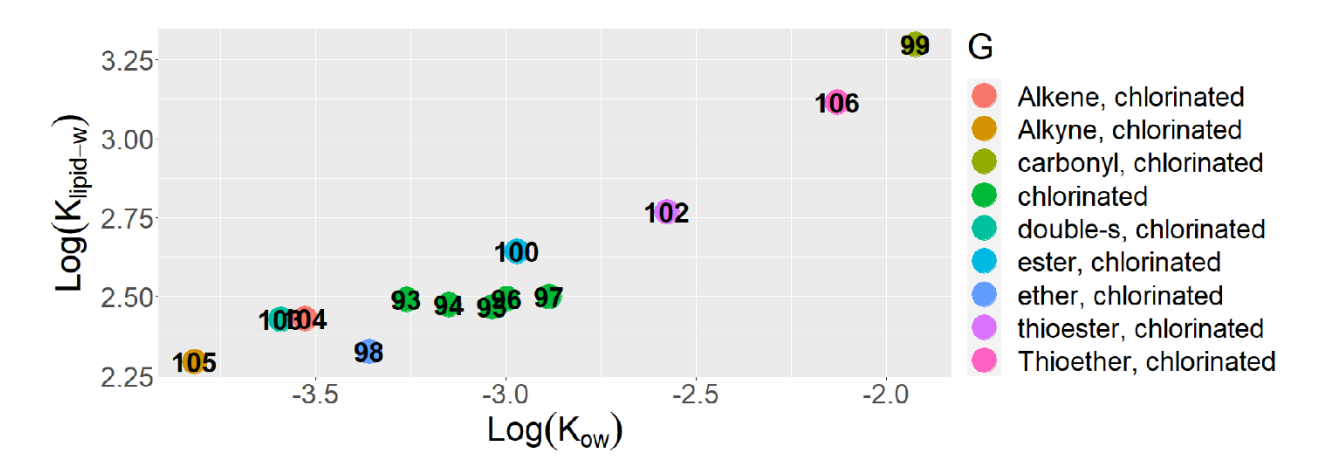


Figure 11: Plot of log  $K_{lipid-w}$  vs. log  $K_{OW}$  of octanoic acids with varying degrees of chlorination. The structures associated with the molecule numbers are contained in the Supporting Information. The units of log  $K_{lipid-w}$  are L(water)/kg(lipid).

The degree of chlorination's impact on the partition coefficients has been visualized in Figure 11. Considering chlorinated analogs of PFOA (molecules #93 to #97) has minimal impact on the log K<sub>lipid-w</sub> value, hovering around 2.50 log units and a range of 0.032 logarithmic units. Log K<sub>OW</sub> values had a larger range of 0.375 logarithmic units. The log K<sub>lipid-w</sub>/log K<sub>OW</sub>/pK<sub>a</sub> value increases as the degree of chlorination increases when comparing the values of these chlorinated analogues to PFOA.

#### 4. Conclusions

In this study, we have conducted geometry optimizations of conformers of 150 different 8-carbon containing poly-/per-fluoroalkyl carboxylic acids (C8-PFCAs) utilizing density functional theory (DFT). From these optimized structures, COnductor like Screening MOdel for Realistic Solvents (COSMO-RS) theory was utilized to predict the acid dissociation constant (pK<sub>a</sub>), the octanol-water partition coefficient (log K<sub>OW</sub>), and DPMC lipid-bilayer-water partition coefficients (log K<sub>lipid-w</sub>) of the C8-PFACs. In reference to perfluorooctanoic acid, the molecules considered in this study are modified with a variety of different functional groups.

While there are outliers, general trends based upon our predicted values can be suggested to help aid experimentalists in the fate/transport of these molecules, provide a guideline in the preliminary risk-assessment of C8-PFACs, and help provide physicochemical properties to aid in the daunting remediation of the environment via engineered solutions. For the molecules considered herein we determined that:

- Functionalization of PFCAs results in a range of pK<sub>a</sub> of  $\approx$ 5 logarithmic units.
- Functionalization of PFCAs results in a range of log  $K_{OW}$  of  $\approx$ 7 logarithmic units.
- Functionalization of PFCAs results in a range of log  $K_{lipid-w}$  of  $\approx 3$  logarithmic units.
- Generally, functionalization α or β to the carboxylic head group had the greatest impact on the value of the predicted physicochemical properties.

We assert that COSMO-RS predictions are a good preliminary tool to help aid in the risk assessment of emerging/unknown PFAS. We aggregate the files utilized in this study on our webpage, available for anyone to utilize. We are in the process of developing an even larger database of PFAS that can be utilized by anyone with access to COSMOtherm. We plan to expand our database beyond the carboxylic headgroup and beyond PFAS only containing 8 carbon atoms. As these results are calculated, we will add the files to our webpage.

# 5. Acknowledgment

The authors acknowledge National Science Foundation (Award #1905274 to DSA, and #1904825 to SMS) and the National Institutes for Health (Award R01 ES032717 and K01 DA056690 to ZF) for support of this research. Any opinions, findings, conclusions, or recommendations expressed in this publication are those of the author(s) and do not necessarily reflect the view of the NSF and the NIH.

#### 6. Funding sources

National Science Foundation Award #1904825 National Science Foundation Award #1905274 National Institutes for Health Award R01 ES032717 National Institutes for Health Award K01 DA056690

#### 7. Associated Content

The Supporting Information is available free of charge at (ADD URL).

Details of how estimates of the relative amount of anions in solutions based upon estimated pK<sub>a</sub> were calculated, a table with the molecule number, SMILES, and skeletal structure, a table with the COSMO-RS estimated properties, plots confirming convergence of physicochemical properties vs. number of conformers included in the calculation, a comparison of anionic form and neutral forms of each molecule, and a summary of the different pKa values from literature are contained within the Supporting Information.

#### 8. References

- (1) Dickman, R. A.; Aga, D. S. A Review of Recent Studies on Toxicity, Sequestration, and Degradation of per- and Polyfluoroalkyl Substances (PFAS). *J. Hazard. Mater.* **2022**, *436*, 129120. https://doi.org/10.1016/j.jhazmat.2022.129120.
- (2) Khan, B.; Burgess, R. M.; Cantwell, M. G. Occurrence and Bioaccumulation Patterns of Per- and Polyfluoroalkyl Substances (PFAS) in the Marine Environment. *ACS EST Water* **2023**, *3* (5), 1243–1259. https://doi.org/10.1021/acsestwater.2c00296.
- (3) Sunderland, E. M.; Hu, X. C.; Dassuncao, C.; Tokranov, A. K.; Wagner, C. C.; Allen, J. G. A Review of the Pathways of Human Exposure to Poly- and Perfluoroalkyl Substances (PFASs) and Present Understanding of Health Effects. *J. Expo. Sci. Environ. Epidemiol.* **2019**, *29* (2), 131–147. https://doi.org/10.1038/s41370-018-0094-1.
- (4) De Silva, A. O.; Spencer, C.; Scott, B. F.; Backus, S.; Muir, D. C. G. Detection of a Cyclic Perfluorinated Acid, Perfluoroethylcyclohexane Sulfonate, in the Great Lakes of North America. *Environ. Sci. Technol.* **2011**, *45* (19), 8060–8066. https://doi.org/10.1021/es200135c.
- (5) Zhang, X.; Xue, L.; Deji, Z.; Wang, X.; Liu, P.; Lu, J.; Zhou, R.; Huang, Z. Effects of Exposure to Per- and Polyfluoroalkyl Substances on Vaccine Antibodies: A Systematic Review and Meta-Analysis Based on Epidemiological Studies. *Environ. Pollut.* 2022, 306, 119442. https://doi.org/10.1016/j.envpol.2022.119442.
- (6) Truong, L.; Rericha, Y.; Thunga, P.; Marvel, S.; Wallis, D.; Simonich, M. T.; Field, J. A.; Cao, D.; Reif, D. M.; Tanguay, R. L. Systematic Developmental Toxicity Assessment of a Structurally Diverse Library of PFAS in Zebrafish. J. Hazard. Mater. 2022, 431, 128615. https://doi.org/10.1016/j.jhazmat.2022.128615.
- (7) Buck, R. C.; Korzeniowski, S. H.; Laganis, E.; Adamsky, F. Identification and Classification of Commercially Relevant Per- and Poly-fluoroalkyl Substances (PFAS). *Integr. Environ. Assess. Manag.* **2021**, *17* (5), 1045–1055. https://doi.org/10.1002/ieam.4450.
- (8) Richard, A. M.; Lougee, R.; Adams, M.; Hidle, H.; Yang, C.; Rathman, J.; Magdziarz, T.; Bienfait, B.; Williams, A. J.; Patlewicz, G. A New CSRML Structure-Based Fingerprint Method for Profiling and Categorizing Per- and Polyfluoroalkyl Substances (PFAS). *Chem. Res. Toxicol.* **2023**, *36* (3), 508–534. https://doi.org/10.1021/acs.chemrestox.2c00403.

- (9) Williams, A. J.; Grulke, C. M.; Edwards, J.; McEachran, A. D.; Mansouri, K.; Baker, N. C.; Patlewicz, G.; Shah, I.; Wambaugh, J. F.; Judson, R. S.; Richard, A. M. The CompTox Chemistry Dashboard: A Community Data Resource for Environmental Chemistry. *J. Cheminformatics* **2017**, *9* (1), 61. https://doi.org/10.1186/s13321-017-0247-6.
- (10) PFAS | EPA: PFAS Structures in DSSTox (Update August 2022) https://comptox.epa.gov/dashboard/chemical-lists/PFASSTRUCTV5 (Accessed November 3, 2023).
- (11) Wang, Z.; DeWitt, J. C.; Higgins, C. P.; Cousins, I. T. A Never-Ending Story of Per- and Polyfluoroalkyl Substances (PFASs)? *Environ. Sci. Technol.* **2017**, *51* (5), 2508–2518. https://doi.org/10.1021/acs.est.6b04806.
- (12) Renner, R. The KOW Controversy. *Environ. Sci. Technol.* **2002**, *36* (21), 410A-413A. https://doi.org/10.1021/es022457+.
- (13) Van Der Spoel, D.; Manzetti, S.; Zhang, H.; Klamt, A. Prediction of Partition Coefficients of Environmental Toxins Using Computational Chemistry Methods. *ACS Omega* **2019**, *4* (9), 13772–13781. https://doi.org/10.1021/acsomega.9b01277.
- (14) Salthammer, T.; Grimme, S.; Stahn, M.; Hohm, U.; Palm, W.-U. Quantum Chemical Calculation and Evaluation of Partition Coefficients for Classical and Emerging Environmentally Relevant Organic Compounds. *Environ. Sci. Technol.* **2022**, *56* (1), 379–391. https://doi.org/10.1021/acs.est.1c06935.
- (15) Hermens, J. L. M.; De Bruijn, J. H. M.; Brooke, D. N. The Octanol-Water Partition Coefficient: Strengths and Limitations. *Environ. Toxicol. Chem.* **2013**, *32* (4), 732–733. https://doi.org/10.1002/etc.2141.
- (16) Charbonnet, J. A.; McDonough, C. A.; Xiao, F.; Schwichtenberg, T.; Cao, D.; Kaserzon, S.; Thomas, K. V.; Dewapriya, P.; Place, B. J.; Schymanski, E. L.; Field, J. A.; Helbling, D. E.; Higgins, C. P. Communicating Confidence of Per- and Polyfluoroalkyl Substance Identification via High-Resolution Mass Spectrometry. *Environ. Sci. Technol. Lett.* **2022**, *9* (6), 473–481. https://doi.org/10.1021/acs.estlett.2c00206.
- (17) De Silva, A. O.; Armitage, J. M.; Bruton, T. A.; Dassuncao, C.; Heiger-Bernays, W.; Hu, X. C.; Kärrman, A.; Kelly, B.; Ng, C.; Robuck, A.; Sun, M.; Webster, T. F.; Sunderland, E. M. PFAS Exposure Pathways for Humans and Wildlife: A Synthesis of Current Knowledge and Key Gaps in Understanding. *Environ. Toxicol. Chem.* **2021**, *40* (3), 631–657. https://doi.org/10.1002/etc.4935.
- (18) Arp, H. P. H.; Droge, S. T. J.; Endo, S.; Giger, W.; Goss, K.-U.; Hawthorne, S. B.; Mabury, S. A.; Mayer, P.; Mclachlan, M. S.; Pankow, J. F.; Schwarzenbach, R. P.; Wania, F.; Xing, B. More of EPA's SPARC Online Calculator—The Need for High-Quality Predictions of Chemical Properties. *Environ. Sci. Technol.* **2010**, *44* (12), 4400–4401. https://doi.org/10.1021/es100437g.
- (19) Goss, K.-U. The p K<sub>a</sub> Values of PFOA and Other Highly Fluorinated Carboxylic Acids. *Environ. Sci. Technol.* **2008**, *42* (2), 456–458. https://doi.org/10.1021/es702192c.
- (20) Wang, Z.; MacLeod, M.; Cousins, I. T.; Scheringer, M.; Hungerbühler, K. Using COSMOtherm to Predict Physicochemical Properties of Poly- and Perfluorinated Alkyl Substances (PFASs). *Environ. Chem.* **2011**, *8* (4), 389. https://doi.org/10.1071/EN10143.
- (21) Arp, H. P. H.; Niederer, C.; Goss, K.-U. Predicting the Partitioning Behavior of Various Highly Fluorinated Compounds. *Environ. Sci. Technol.* **2006**, *40* (23), 7298–7304. https://doi.org/10.1021/es060744y.
- (22) Lawler, R.; Liu, Y.-H.; Majaya, N.; Allam, O.; Ju, H.; Kim, J. Y.; Jang, S. S. DFT-Machine Learning Approach for Accurate Prediction of p *K* <sub>a</sub>. *J. Phys. Chem. A* **2021**, *125* (39), 8712–8722. https://doi.org/10.1021/acs.jpca.1c05031.
- (23) Endo, S.; Hammer, J.; Matsuzawa, S. Experimental Determination of Air/Water Partition Coefficients for 21 Per- and Polyfluoroalkyl Substances Reveals Variable Performance of Property Prediction Models. *Environ. Sci. Technol.* **2023**, *57* (22), 8406–8413. https://doi.org/10.1021/acs.est.3c02545.

- (24) Lampic, A.; Parnis, J. M. Property Estimation of Per- and Polyfluoroalkyl Substances: A Comparative Assessment of Estimation Methods. *Environ. Toxicol. Chem.* **2020**, *39* (4), 775–786. https://doi.org/10.1002/etc.4681.
- (25) Zhang, M.; Suuberg, E. M. Estimation of Vapor Pressures of Perfluoroalkyl Substances (PFAS) Using COSMOtherm. *J. Hazard. Mater.* **2023**, *443*, 130185. https://doi.org/10.1016/j.jhazmat.2022.130185.
- (26) Sima, M. W.; Jaffé, P. R. A Critical Review of Modeling Poly- and Perfluoroalkyl Substances (PFAS) in the Soil-Water Environment. *Sci. Total Environ.* **2021**, *757*, 143793. https://doi.org/10.1016/j.scitotenv.2020.143793.
- (27) Lai, T. T.; Kuntz, D.; Wilson, A. K. Molecular Screening and Toxicity Estimation of 260,000 Perfluoroalkyl and Polyfluoroalkyl Substances (PFASs) through Machine Learning. *J. Chem. Inf. Model.* **2022**, *62* (19), 4569–4578. https://doi.org/10.1021/acs.jcim.2c00374.
- (28) Kim, S.-K.; Li, D.; Kannan, K. *In Situ* Measurement-Based Partitioning Behavior of Perfluoroalkyl Acids in the Atmosphere. *Environ. Eng. Res.* **2019**, *25* (3), 281–289. https://doi.org/10.4491/eer.2019.130.
- (29) Namazian, M.; Zakery, M.; Noorbala, M. R.; Coote, M. L. Accurate Calculation of the pKa of Trifluoroacetic Acid Using High-Level Ab Initio Calculations. *Chem. Phys. Lett.* **2008**, *451* (1–3), 163–168. https://doi.org/10.1016/j.cplett.2007.11.088.
- (30) Reinisch, J.; Diedenhofen, M.; Wilcken, R.; Udvarhelyi, A.; Glöß, A. Benchmarking Different QM Levels for Usage with COSMO-RS. *J. Chem. Inf. Model.* **2019**, *59* (11), 4806–4813. https://doi.org/10.1021/acs.jcim.9b00659.
- (31) Sülzner, N.; Haberhauer, J.; Hättig, C.; Hellweg, A. Prediction of Acid p K a Values in the Solvent Acetone Based on COSMO-RS. *J. Comput. Chem.* **2022**, *43* (15), 1011–1022. https://doi.org/10.1002/jcc.26864.
- (32) Klamt, A. The COSMO and COSMO-RS Solvation Models. *WIREs Comput. Mol. Sci.* **2018**, *8* (1), e1338. https://doi.org/10.1002/wcms.1338.
- (33) Müller, K.; Faeh, C.; Diederich, F. Fluorine in Pharmaceuticals: Looking Beyond Intuition. *Science* **2007**, *317* (5846), 1881–1886. https://doi.org/10.1126/science.1131943.
- (34) Shen, Z.; Ge, J.; Ye, H.; Tang, S.; Li, Y. Cholesterol-like Condensing Effect of Perfluoroalkyl Substances on a Phospholipid Bilayer. *J. Phys. Chem. B* **2020**, *124* (26), 5415–5425. https://doi.org/10.1021/acs.jpcb.0c00980.
- (35) Gomis, M. I.; Wang, Z.; Scheringer, M.; Cousins, I. T. A Modeling Assessment of the Physicochemical Properties and Environmental Fate of Emerging and Novel Per- and Polyfluoroalkyl Substances. *Sci. Total Environ.* **2015**, *505*, 981–991. https://doi.org/10.1016/j.scitotenv.2014.10.062.
- (36) Wang, Z.; Cousins, I. T.; Scheringer, M.; Hungerbuehler, K. Hazard Assessment of Fluorinated Alternatives to Long-Chain Perfluoroalkyl Acids (PFAAs) and Their Precursors: Status Quo, Ongoing Challenges and Possible Solutions. *Environ. Int.* **2015**, *75*, 172–179. https://doi.org/10.1016/j.envint.2014.11.013.
- (37) Zweigle, J.; Bugsel, B.; Capitain, C.; Zwiener, C. PhotoTOP: PFAS Precursor Characterization by UV/TiO <sub>2</sub> Photocatalysis. *Environ. Sci. Technol.* **2022**, *56* (22), 15728–15736. https://doi.org/10.1021/acs.est.2c05652.
- (38) Zweigle, J.; Bugsel, B.; Röhler, K.; Haluska, A. A.; Zwiener, C. PFAS-Contaminated Soil Site in Germany: Nontarget Screening before and after Direct TOP Assay by Kendrick Mass Defect and FindPFΔS. *Environ. Sci. Technol.* **2023**, *57* (16), 6647–6655. https://doi.org/10.1021/acs.est.2c07969.
- (39) Thompson, J. T.; Robey, N. M.; Tolaymat, T. M.; Bowden, J. A.; Solo-Gabriele, H. M.; Townsend, T. G. Underestimation of Per- and Polyfluoroalkyl Substances in Biosolids: Precursor Transformation During Conventional Treatment. *Environ. Sci. Technol.* **2023**, *57* (9), 3825–3832. https://doi.org/10.1021/acs.est.2c06189.

- (40) Pickard, H. M.; Ruyle, B. J.; Thackray, C. P.; Chovancova, A.; Dassuncao, C.; Becanova, J.; Vojta, S.; Lohmann, R.; Sunderland, E. M. PFAS and Precursor Bioaccumulation in Freshwater Recreational Fish: Implications for Fish Advisories. *Environ. Sci. Technol.* **2022**, *56* (22), 15573–15583. https://doi.org/10.1021/acs.est.2c03734.
- (41) McDonough, C. A.; Li, W.; Bischel, H. N.; De Silva, A. O.; DeWitt, J. C. Widening the Lens on PFASs: Direct Human Exposure to Perfluoroalkyl Acid Precursors (Pre-PFAAs). *Environ. Sci. Technol.* **2022**, 56 (10), 6004–6013. https://doi.org/10.1021/acs.est.2c00254.
- (42) Droge, S. T. J. Membrane–Water Partition Coefficients to Aid Risk Assessment of Perfluoroalkyl Anions and Alkyl Sulfates. *Environ. Sci. Technol.* **2019**, *53* (2), 760–770. https://doi.org/10.1021/acs.est.8b05052.
- (43) Goss, K.-U.; Arp, H. P. H. Comment on "Experimental p K<sub>a</sub> Determination for Perfluorooctanoic Acid (PFOA) and the Potential Impact of p K<sub>a</sub> Concentration Dependence on Laboratory-Measured Partitioning Phenomena and Envrionmental Modeling." *Environ. Sci. Technol.* **2009**, *43* (13), 5150–5151. https://doi.org/10.1021/es900451s.
- (44) Burns, D. C.; Ellis, D. A.; Li, H.; McMurdo, C. J.; Webster, E. Experimental p K<sub>a</sub> Determination for Perfluorooctanoic Acid (PFOA) and the Potential Impact of p K<sub>a</sub> Concentration Dependence on Laboratory-Measured Partitioning Phenomena and Environmental Modeling. *Environ. Sci. Technol.* **2008**, *42* (24), 9283–9288. https://doi.org/10.1021/es802047v.
- (45) Ellis, D. A.; Webster, E. Response to Comment on "Aerosol Enrichment of the Surfactant PFO and Mediation of the Water–Air Transport of Gaseous PFOA." *Environ. Sci. Technol.* **2009**, *43* (4), 1234–1235. https://doi.org/10.1021/es8033654.
- (46) Bittermann, K.; Spycher, S.; Goss, K.-U. Comparison of Different Models Predicting the Phospholipid-Membrane Water Partition Coefficients of Charged Compounds. *Chemosphere* 2016, 144, 382–391. https://doi.org/10.1016/j.chemosphere.2015.08.065.
- (47) Meylan, W. M.; Howard, P. H.; Boethling, R. S.; Aronson, D.; Printup, H.; Gouchie, S. Improved Method for Estimating Bioconcentration/Bioaccumulation Factor from Octanol/Water Partition Coefficient. *Environ. Toxicol. Chem.* **1999**, *18* (4), 664–672. https://doi.org/10.1002/etc.5620180412.
- (48) Geyer, H.; Politzki, G.; Freitag, D. Prediction of Ecotoxicological Behaviour of Chemicals: Relationship between n-Octanol/Water Partition Coefficient and Bioaccumulation of Organic Chemicals by Alga. *Chemosphere* **1984**, *13* (2), 269–284. https://doi.org/10.1016/0045-6535(84)90134-6.
- (49) Czerwinski, S. E.; Skvorak, J. P.; Maxwell, D. M.; Lenz, D. E.; Baskin, S. I. Effect of Octanol:Water Partition Coefficients of Organophosphorus Compounds on Biodistribution and Percutaneous Toxicity. *J. Biochem. Mol. Toxicol.* **2006**, *20* (5), 241–246. https://doi.org/10.1002/jbt.20140.
- (50) Shi, J.-Q.; Cheng, J.; Wang, F.-Y.; Flamm, A.; Wang, Z.-Y.; Yang, X.; Gao, S.-X. Acute Toxicity and N-Octanol/Water Partition Coefficients of Substituted Thiophenols: Determination and QSAR Analysis. *Ecotoxicol. Environ. Saf.* **2012**, *78*, 134–141. https://doi.org/10.1016/j.ecoenv.2011.11.024.
- (51) Fitzgerald, N. J. M.; Wargenau, A.; Sorenson, C.; Pedersen, J.; Tufenkji, N.; Novak, P. J.; Simcik, M. F. Partitioning and Accumulation of Perfluoroalkyl Substances in Model Lipid Bilayers and Bacteria. *Environ. Sci. Technol.* **2018**, *52* (18), 10433–10440. https://doi.org/10.1021/acs.est.8b02912.
- (52) Lv, G.; Sun, X. The Molecular-Level Understanding of the Uptake of PFOS and Its Alternatives (6:2 Cl-PFESA and OBS) into Phospholipid Bilayers. *J. Hazard. Mater.* **2021**, *417*, 125991. https://doi.org/10.1016/j.jhazmat.2021.125991.
- (53) Ebert, A.; Allendorf, F.; Berger, U.; Goss, K.-U.; Ulrich, N. Membrane/Water Partitioning and Permeabilities of Perfluoroalkyl Acids and Four of Their Alternatives and the Effects on Toxicokinetic Behavior. *Environ. Sci. Technol.* **2020**, *54* (8), 5051–5061. https://doi.org/10.1021/acs.est.0c00175.
- (54) Ingram, T.; Storm, S.; Kloss, L.; Mehling, T.; Jakobtorweihen, S.; Smirnova, I. Prediction of Micelle/Water and Liposome/Water Partition Coefficients Based on Molecular Dynamics

- Simulations, COSMO-RS, and COSMOmic. *Langmuir* **2013**, *29* (11), 3527–3537. https://doi.org/10.1021/la305035b.
- (55) Armitage, J. M.; Arnot, J. A.; Wania, F. Potential Role of Phospholipids in Determining the Internal Tissue Distribution of Perfluoroalkyl Acids in Biota. *Environ. Sci. Technol.* **2012**, *46* (22), 12285–12286. https://doi.org/10.1021/es304430r.
- (56) Dassuncao, C.; Pickard, H.; Pfohl, M.; Tokranov, A. K.; Li, M.; Mikkelsen, B.; Slitt, A.; Sunderland, E. M. Phospholipid Levels Predict the Tissue Distribution of Poly- and Perfluoroalkyl Substances in a Marine Mammal. *Environ. Sci. Technol. Lett.* 2019, 6 (3), 119–125. https://doi.org/10.1021/acs.estlett.9b00031.
- (57) Hanwell, M. D.; Curtis, D. E.; Lonie, D. C.; Vandermeersch, T.; Zurek, E.; Hutchison, G. R. Avogadro: An Advanced Semantic Chemical Editor, Visualization, and Analysis Platform. *J. Cheminformatics* **2012**, *4* (1), 17. https://doi.org/10.1186/1758-2946-4-17.
- (58) Chang, C.-E.; Gilson, M. K. Tork: Conformational Analysis Method for Molecules and Complexes. *J. Comput. Chem.* **2003**, *24* (16), 1987–1998. https://doi.org/10.1002/jcc.10325.
- (59) Balasubramani, S. G.; Chen, G. P.; Coriani, S.; Diedenhofen, M.; Frank, M. S.; Franzke, Y. J.; Furche, F.; Grotjahn, R.; Harding, M. E.; Hättig, C.; Hellweg, A.; Helmich-Paris, B.; Holzer, C.; Huniar, U.; Kaupp, M.; Marefat Khah, A.; Karbalaei Khani, S.; Müller, T.; Mack, F.; Nguyen, B. D.; Parker, S. M.; Perlt, E.; Rappoport, D.; Reiter, K.; Roy, S.; Rückert, M.; Schmitz, G.; Sierka, M.; Tapavicza, E.; Tew, D. P.; Van Wüllen, C.; Voora, V. K.; Weigend, F.; Wodyński, A.; Yu, J. M. TURBOMOLE: Modular Program Suite for *Ab Initio* Quantum-Chemical and Condensed-Matter Simulations. *J. Chem. Phys.* 2020, 152 (18), 184107. https://doi.org/10.1063/5.0004635.
- (60) TURBOMOLE V7.3 2018, a development of University of Karlsruhe and Forschungszentrum Karlsruhe GmbH, 1989-2007, TURBOMOLE GmbH, since 2007; available from http://www.turbomole.com.
- (61) Becke, A. D. Density-Functional Exchange-Energy Approximation with Correct Asymptotic Behavior. *Phys. Rev. A* **1988**, *38* (6), 3098–3100. https://doi.org/10.1103/PhysRevA.38.3098.
- (62) Schäfer, A.; Huber, C.; Ahlrichs, R. Fully Optimized Contracted Gaussian Basis Sets of Triple Zeta Valence Quality for Atoms Li to Kr. *J. Chem. Phys.* **1994**, *100* (8), 5829–5835. https://doi.org/10.1063/1.467146.
- (63) COSMOtherm. https://www.3ds.com/products-services/biovia/products/molecular-modeling-simulation/solvation-chemistry/biovia-cosmotherm/ (accessed 2023-06-20).
- (64) Klamt, A. COSMO-RS; Elsevier Science, 2005.
- (65) Klamt, A. Conductor-like Screening Model for Real Solvents: A New Approach to the Quantitative Calculation of Solvation Phenomena. *J. Phys. Chem.* **1995**, *99* (7), 2224–2235. https://doi.org/10.1021/j100007a062.
- (66) Klamt, A.; Jonas, V.; Bürger, T.; Lohrenz, J. C. W. Refinement and Parametrization of COSMO-RS. *J. Phys. Chem. A* **1998**, *102* (26), 5074–5085. https://doi.org/10.1021/jp980017s.
- (67) Guardian, M. G. E.; Antle, J. P.; Vexelman, P. A.; Aga, D. S.; Simpson, S. M. Resolving Unknown Isomers of Emerging Per- and Polyfluoroalkyl Substances (PFASs) in Environmental Samples Using COSMO-RS-Derived Retention Factor and Mass Fragmentation Patterns. J. Hazard. Mater. 2021, 402, 123478. https://doi.org/10.1016/j.jhazmat.2020.123478.
- (68) Klamt, A.; Eckert, F.; Diedenhofen, M.; Beck, M. E. First Principles Calculations of Aqueous p K<sub>a</sub> Values for Organic and Inorganic Acids Using COSMO–RS Reveal an Inconsistency in the Slope of the p K<sub>a</sub> Scale. *J. Phys. Chem. A* **2003**, *107* (44), 9380–9386. https://doi.org/10.1021/jp0346880.
- (69) Armitage, J. M.; MacLeod, M.; Cousins, I. T. Modeling the Global Fate and Transport of Perfluorooctanoic Acid (PFOA) and Perfluorooctanoate (PFO) Emitted from Direct Sources Using a Multispecies Mass Balance Model. *Environ. Sci. Technol.* 2009, 43 (4), 1134–1140. https://doi.org/10.1021/es802900n.

- (70) Moroi, Y.; Yano, H.; Shibata, O.; Yonemitsu, T. Determination of Acidity Constants of Perfluoroalkanoic Acids. *Bull. Chem. Soc. Jpn.* **2001**, *74* (4), 667–672. https://doi.org/10.1246/bcsj.74.667.
- (71) Čabala, R.; Nesměrák, K.; Vlasáková, T. Dissociation Constants of Perfluoroalkanoic Acids. Monatshefte Für Chem. - Chem. Mon. 2017, 148 (9), 1679–1684. https://doi.org/10.1007/s00706-017-1970-4.
- (72) Klamt, A.; Huniar, U.; Spycher, S.; Keldenich, J. COSMOmic: A Mechanistic Approach to the Calculation of Membrane–Water Partition Coefficients and Internal Distributions within Membranes and Micelles. *J. Phys. Chem. B* **2008**, *112* (38), 12148–12157. https://doi.org/10.1021/jp801736k.
- (73) Jakobtorweihen, S.; Ingram, T.; Smirnova, I. Combination of COSMOmic and Molecular Dynamics Simulations for the Calculation of Membrane-Water Partition Coefficients. *J. Comput. Chem.* **2013**, *34* (15), 1332–1340. https://doi.org/10.1002/jcc.23262.
- (74) Bittermann, K.; Spycher, S.; Endo, S.; Pohler, L.; Huniar, U.; Goss, K.-U.; Klamt, A. Prediction of Phospholipid–Water Partition Coefficients of Ionic Organic Chemicals Using the Mechanistic Model COSMO *Mic. J. Phys. Chem. B* **2014**, *118* (51), 14833–14842. https://doi.org/10.1021/jp509348a.
- (75) Carmosini, N.; Lee, L. S. Partitioning of Fluorotelomer Alcohols to Octanol and Different Sources of Dissolved Organic Carbon. *Environ. Sci. Technol.* **2008**, *42* (17), 6559–6565. https://doi.org/10.1021/es800263t.
- (76) Igarashi, S.; Yotsuyanagi, T. Homogeneous Liquid-Liquid Extraction by pH Dependent Phase Separation with a Fluorocarbon Ionic Surfactant and Its Application to the Preconcentration of Porphyrin Compounds. *Mikrochim. Acta* **1992**, *106* (1–2), 37–44. https://doi.org/10.1007/BF01242697.
- (77) López-Fontán, J. L.; Sarmiento, F.; Schulz, P. C. The Aggregation of Sodium Perfluorooctanoate in Water. *Colloid Polym. Sci.* **2005**, *283* (8), 862–871. https://doi.org/10.1007/s00396-004-1228-7.
- (78) Hoffmann, R.; Schleyer, P. von R.; Schaefer, H. F. Predicting Molecules-More Realism, Please! *Angew. Chem. Int. Ed.* **2008**, *47* (38), 7164–7167. https://doi.org/10.1002/anie.200801206.
- (79) Simpson, S. *PFAS COSMO-RS Files*. https://sites.google.com/view/simpson-research/pfas-cosmo-rs-files. (Accessed November 3, 2023).

# TABLE OF CONTENTS GRAPHIC

